Meteorol Atmos Phys 84, 229–242 (2003)
DOI 10.1007/s00703-003-0001-7

Meteorology and Atmospheric Physics
Printed in Austria

[1] Department of Mathematical Sciences, Atmospheric Sciences Group, University of Wisconsin-Milwaukee, Milwaukee
[2] CIRES, University of Colorado, Boulder
[3] Department of Geography, Florida State University, Tallahassee

On the relation between ENSO and global climate change

A. A. Tsonis[1], **A. G. Hunt**[2], and **J. B. Elsner**[3]

With 8 Figures

Revised November 14, 2002; accepted November 28, 2002
Published online: June 12, 2003 © Springer-Verlag 2003

Summary

Two lines of research into climate change and El Niño/Southern Oscillation (ENSO) converge on the conclusion that changes in ENSO statistics occur as a response to global climate (temperature) fluctuations. One approach focuses on the statistics of temperature fluctuations interpreted within the framework of random walks. The second is based on the discovery of correlation between the recurrence frequency of El Niño and temperature change, while developing physical arguments to explain several phenomena associated with changes in El Niño frequency. Consideration of both perspectives leads to greater confidence in, and guidance for, the physical interpretation of the relationship between ENSO and global climate change. Topics considered include global dynamics of ENSO, ENSO triggers, and climate prediction and predictability.

1. Introduction

The dynamics of El Niño are understood in terms of a combination of concepts from stochastic and deterministic theoretical approaches. The Wyrtki (1975) approach is predominantly stochastic in character, and describes the trigger of El Niño in terms of stronger than usual trade winds (and larger than usual sea surface elevation gradients) followed by anomalous relaxation of trade winds. The most important concept from the recent deterministic models of El Niño appears to be the "memory paradigm," whereby the western equatorial and off-equatorial Pacific Ocean upper layer carries a memory of up to 2 years of trade wind stresses, equatorial upwelling, solar heating, and convective and radiative cooling (Neelin et al, 1998). Taken together, these two ideas form the basis for interpretation of the effects of climate change on El Niño.

Under normal conditions, the Walker circulation drives easterly trade winds. The northeasterly (southeasterly) winds in the northern (southern) hemisphere move surface water westward across the equatorial Pacific. The Coriolis effect causes surface water divergence along the equator with the result that, on both sides of the equator, water is driven up onto the subtropical gyres. In response to the surface divergence, equatorial upwelling replaces warmer surface water with cooler water from below the thermocline. The effects of this equatorial upwelling are enhanced by the geographical connection with coastal upwelling off the coast of South America. The long residence time in the tropics of water driven up on to the subtropical gyres and transported to the western equatorial Pacific allows these surface waters to heat up relative to the central and eastern equatorial Pacific (where the upwelling is taking place) resulting in an equatorial "cold tongue" with warmer water to the west, north and south, in a shape resembling a

horseshoe. The areas with warmer water (also higher by tens of centimeters) are supported by an unusually deep thermocline (Philander, 1990), and held in place by the competition between pressure and wind stress. The eastern equatorial Pacific sea surface is close to equilibrium with the wind stress (Schneider et al, 1995). Because of that, strong easterlies produce significant upwelling and cold surface temperatures (at times less than 20 °C) while weak easterlies or westerlies suppress upwelling allowing the development of warm surface temperatures (as warm as 28 °C) along the equator.

The western equatorial (and off-equatorial) Pacific sea surface is not in equilibrium with wind stress (Neelin et al, 1998). As a result, changes in winds produce changes to the depth of the thermocline, but the surface is nearly always at 28–30 °C. The warmer water in the western Pacific is associated with strong convection (which takes place over water warmer than 28 °C). The convection is a positive feedback that leads to enhanced trade winds, and (on average) a return of air aloft to the eastern Pacific. This circulation is named after Walker, who first noticed large-scale shifts in it (Walker, 1923; 1924). The general sea surface topography has, in the mean state, a "groove" along the equator deepening to the east, with small hills north and south, and is highest toward the west. This configuration is unstable to prolonged westerly wind anomalies. The region is unique in that convergent (westerly) surface winds produce convergent (easterly) surface ocean currents as noted in Philander (1990). When westerly wind anomalies occur, warm water flows off both subtropical gyres (Tziperman et al, 1998) and from the west into the central equatorial Pacific. A Kelvin wave may be triggered, with its associated increase in depth to the thermocline. A feedback induced by eastward displacement of warm surface water and associated convection can enhance westerly wind anomalies.

The precise generation of El Niño is still uncertain, with considerable discussion regarding the relative roles of the interrelated factors (wind, SSTs, upwelling) and the mechanisms for propagating and sustaining the warm anomaly. Clearly, some variability in the generation of El Niño exists as well. But, in general, it is widely accepted that the trigger of El Niño is a combination of anomalous westerly wind bursts (Wyrtki, 1975; McPhaden, 1999; Yu and Rienecker, 1998), equatorial Pacific SST gradient, and sufficient heat energy, which through positive feedback of convection can be spread around the surface of the entire equatorial Pacific (Neelin et al, 1998). These changes are linked to the atmospheric circulation locally and through much of the rest of the world through teleconnections. Because the anomalous ocean warming and the sea surface pressure reversals occur simultaneously, the whole phenomenon is called El Niño/Southern Oscillation (ENSO). When El Niño dies out, the tendency is for trade winds to return to normal or even exceed normal. If, however, they become too strong, then the cold-water pool normally found in the eastern Pacific stretches farther westward than normal and the warm water is confined to the western tropical Pacific. This opposite to El Niño is called La Niña.

ENSO is generally considered to have its largest influence on weather patterns and climate fluctuations over inter-annual time scales. Winter weather patterns over specific areas of the globe are now routinely predicted with some confidence on the basis of tropical sea surface temperature (SST) anomalies associated with El Niño, as well as SST's in temperate oceans. El Niño, and its opposite, La Niña, tend to last between 1 and 2 years. In fact, however, the 1940–1942, the 1976–1978, and the 1990–1993 El Niño events, each persisted through at least two winters, and the recent La Niña lasted two winters, persisting weakly into a third. The existence of multi-winter events probably plays a role in the success of persistence as a forecast tool, i.e. reference to the preceding winter, for predicting the weather during the next winter. The typical period of time between El Niño events is approximately 4 years. The typical time between La Niña events is probably the same, or nearly so, but the statistical record of La Niña is more limited, introducing a greater uncertainty.

The influence of climate change on El Niño is less well understood and subject to some controversy (Solow, 1995; Trenberth and Hoar, 1997; Rajagopalan et al, 1997; Tsonis et al, 1998; Hunt, 1999a, b). The controversy concerns the roles of stochastic forcing and nonlinearity in the dynamics and on the statistics of El Niño (Wang and Wang, 1996; Kestin et al, 1998; Blanke

et al, 1997; Tziperman et al, 1997; Hunt, 1999a, b; Hunt, 2000). Nevertheless, evidence presented here is convincing in depth and scope, that global surface temperatures strongly influence El Niño. In particular, periods of rising temperature encourage El Niño events, while periods of decreasing temperature encourage La Niña events. While both appear to occur approximately 1 year in 4 when global temperatures remain constant, during periods of rising temperature, El Niño events occur as often as 1 year in 2.5, whereas La Niña events occur as seldom as 1 year in 7. In contrast, during periods of decreasing temperature, El Niño events occur as seldom as 1 year in 7, whereas La Niña events occur as often as 1 year in 3. Since global temperatures tend to fall after an El Niño, but rise after a La Niña, the cycle of El Niño-La Niña can, from the perspective of climate change, be regarded as a negative feedback mechanism. This view is put on firm statistical grounds by an analysis of the global temperature record in terms of a correlated random walk (Tsonis et al, 1998). Moreover, the conceptual framework of Hunt (1999b) provides a physical explanation to the statistical analysis. Note that here the term global change is used in general. Whether the observed global change over the past century is due to greenhouse warming or natural variability is not of concern to the theory.

2. Correlating ENSO with global temperature records

For investigating statistics of El Niño one can choose between using the last 100 years or so of nearly unambiguous records or consider a much larger time scale with attendant uncertainties. The former choice is not practical here because only two periods of distinct temperature change exist, which is insufficient for the analysis. The latter choice carries with it the disadvantage that both the temperature record and the record of occurrence of El Niño can be criticized as inaccurate, incomplete, or of uncertain resolution. Nevertheless, the consistency of the picture that emerges makes the individual data sources appear more reliable. While the climatic signal of La Niña events is difficult to detect at times in the past, the teleconnections of El Niño are more easily detectable, and several studies have been performed to reconstruct the past occurrence of El Niño. These studies are based variously on coral mortality (Evans et al, 1999; Hughen et al, 1999), flooding in normally arid regions (Rodbell et al, 1999), and the regular Nile River flooding (Anderson, 1992; Quinn, 1992). El Niño, by shifting the position of the Walker circulation, tends to produce increased precipitation in northeastern Africa, causing amplification of the regular Nile River flooding. Here we use data from Quinn (1992) for analysis of the El Niño signal (which uses records from Peru supplemented by records of Nile River flooding).

For long-term temperature records borehole data are most reliable, and are less influenced by subjective interpretation (Pollack and Huang, 1998). Contamination from changes in surfaces or to groundwater, however, is a potential problem. Paleo-temperatures are extracted from borehole data through near-surface alterations in the geothermal gradient (Pollack and Huang, 1998). The earth's temperature normally increases linearly with depth. Changes in surface temperatures propagate slowly downward. A steadily rising atmospheric temperature can induce a sign change in the geothermal gradient near the surface, but will, in any case, produce a curvature between an altered value at the surface and unaffected values at depth (many tens of meters in the case of climate change starting as early as 500 years ago). For the temperature data from the 16th through the 19th centuries we refer to (Pollack and Huang, 1998). These data lack the resolution of the recent temperature data, and are supplemented by the IPCC global temperature data (Folland et al, 1990) from the end of the 19th century to the present. Figure 1 shows the borehole data from (Pollack and Huang, 1998) (thick solid line with shaded uncertainty limits), with the temperature data for the 20th century superimposed. On the same graph the accumulated El Niño events from Quinn (1992) are also plotted. Each upward step is one El Niño event. The thin straight line is the long-term average.

Comparing the cumulative frequency of El Niño occurrence with a reconstruction of global temperatures is equivalent to comparing the occurrence of El Niño with the rate of change of atmospheric temperatures. In order to investigate such a relation we start by observing that breaks in temperature slope (dT/dt) appear at

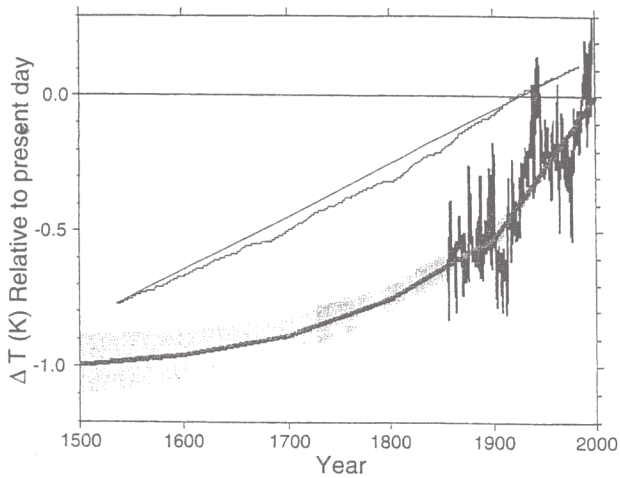

Fig. 1. Direct comparison of cumulative frequency of El Niño occurrence (Quinn, 1992) with global temperature proxy (Evans et al, 1999). Every upward step on the staircase is an El Niño. The yearly averages for global temperature anomaly in the 20th century (Folland et al, 1990) are also shown. Whenever the rate of temperature increase accelerates, at approximately the turns of the centuries, so does the rate of El Niño accumulation

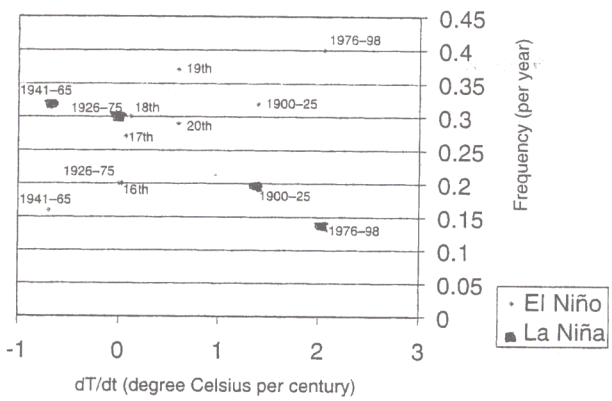

Fig. 2. Relationship between occurrence frequencies (yr^{-1}) of El Niño and La Niña and global temperature change rate, dT/dt (°C/yr). Five individual points taken from Pollack and Huang (1998) compilation of borehole data, and Quinn's reconstruction of El Niño occurrence for the 16th through 20th centuries. The remainder points are from the higher resolution SOI and IPCC data in the 20th century, and correspond to periods of rising, falling, and steady T (see text for details)

approximately the turn of each century. Therefore, 100-year intervals are chosen and the El Niño frequency per year is estimated (Fig. 2), along with the corresponding dT/dt. This results in five points. Due to the better accuracy and resolution of the Southern Oscillation Index (SOI) data and of the global temperature data (IPCC) in the 20th century, we then consider the following additional intervals that mark significantly different dT/dt regimes. The first (1900–1925) is associated with rising T, the second (1926–1975) is characterized by an overall zero trend, and the third (1976–1998) is associated with rising T. An additional interval (1941–1965), which is characterized by a negative trend, is also considered. The choice of these intervals reflects our desire to consider periods where all trend types (positive, zero, and negative) are represented. In Fig. 2, the frequency of occurrence of El Niño in each century is plotted against dT/dt for that century. In the same figure statistics for La Niña events derived from the SOI index during the 20th century and for the abovementioned intervals are included. It is important to stress here that the frequency of El Niño and La Niña is sensitive to the definition of these events. Nevertheless, despite this and other uncertainties inherent in the data considered in the construction of this plot, a rather solid picture emerges. The data appear consistent with a nearly linear relationship between the occurrence of El Niño and La Niña and the global dT/dt. Interestingly, this linearity is characterized by a positive trend for El Niño and a negative trend for La Niña. Such results are not derived when the frequencies of El Niño and La Niña occurrences are plotted against the mean T in the corresponding intervals. In this case (see Fig. 3) the linear relationships observed in Fig. 2 are not evident. In fact no clear relationship is apparent. Note that because the temperature data in the 16th, 17th,

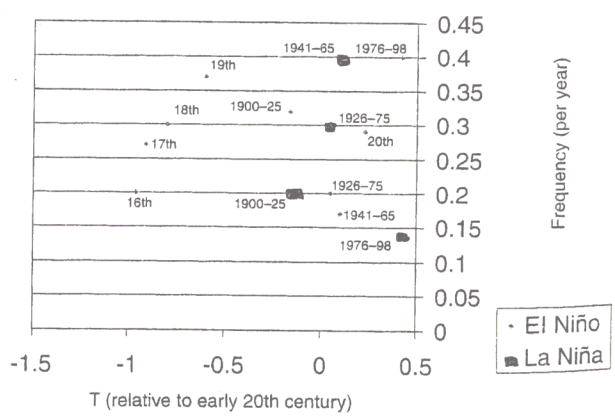

Fig. 3. Same as Fig. 2, but now the occurrence frequencies are plotted against the mean temperature in the corresponding interval

18th, and 19th centuries follow a nearly exponential function, the corresponding points are similar in both graphs. Nevertheless, no solid picture emerges in this case when the rest of the data are included.

The results in Figs. 2 and 3 would then suggest that the frequency of occurrence of El Niño and La Niña depends on *changes* of T, but it is a very weak function of T (i.e., if T were static, the magnitude of T would not significantly affect El Niño/La Niña frequencies). Such a conclusion is in accord with studies of El Niño variability on longer time scales. Rodbell et al (1999), found that the frequency of El Niño events (measured at average values of temperature) increased only from 0.07 to 0.17 with increases in global T of 6 °C. By extrapolation one would conclude that a 20th century increase of global T of 0.6 °C, would result in an increase in the frequency of El Niño of only 0.16 to 0.17, which would be difficult to measure. Further, a similarity in the frequency of El Niño events during the previous interglacial period to that presently observed has recently been claimed (Hughen et al, 1999), despite the fact that global temperatures were notably warmer. Global climate model simulations also appear to support the above conclusion. Recent studies have indicated that a much higher global temperature is required to significantly change the frequency of El Niño (Timmermann et al, 1999a, b; Collins, 2000). Thus results from observations and models indicate that El Niño frequency is, at best, a weak function of temperature. In agreement with our results GCM simulations reproduce this observed relationship between increases in global temperature and increased El Niño frequency. As an example, Fig. 4 shows a time series of the Niño 3 + 4 index (SST averaged 5N–5S, 140E–140W) from a 130 year run of NCAR's CSM1 model in which the CO_2-concentration is increased 1%/year from its pre-industrial level (case b006, data accessible at www.cgd.ucar.edu/csm/experiments/b006). In a steady-state experiment (case b003, data available as above), statistics accumulated over a 300 year model run show that El Niño and La Niña events occur at roughly the same frequency, roughly 17/century, where an event is defined as greater than a one standard deviation departure from the mean, and persistence of at least 6 months. However, in the increasing

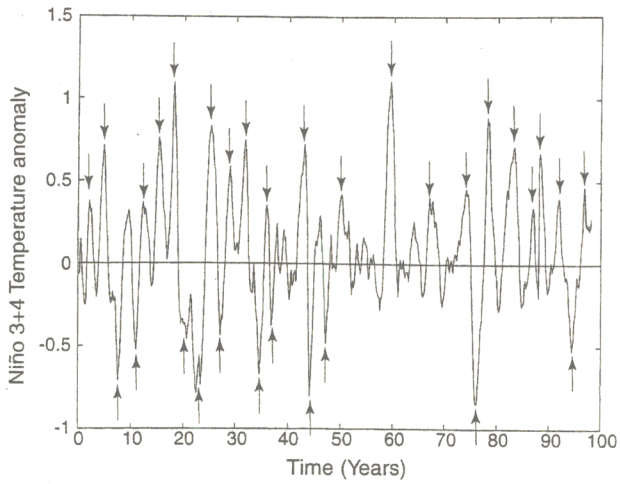

Fig. 4. Time series of the Niño 3 + 4 index (SST averaged 5N–5S, 140E–140W) from a 130 year run of NCAR's CSM1 model in which the CO_2-concentration is increased 1%/year from its pre-industrial level. In this increasing CO_2-experiment, the El Niño frequency is 22/century, while the La Niña frequency drops to 12/century (see text for details)

CO_2-experiment, the El Niño frequency is 20/century, while the La Niña frequency drops to 11/century. This suggests that the influence of global temperature change can be captured by modern coupled GCMs, and that properly designed experiments should allow for an in-depth understanding of why the shift in frequency in El Niño (La Niña) events occurs when global temperatures increase (decrease).

Returning to Fig. 2, it may be suggested that the observed linearity does not extend to values of dT/dt greater than 1 °C/100yr, where El Niño occurrence may saturate at about 0.4/year. The indication of saturation in El Niño occurrence frequency (0.4/yr) below the statistical limit (1/yr) hints that a physical limit is reached. This is supported by the fact that El Niño typically lasts about 18 months and the fact that at least a year is required to generate the heat storage after depletion by the previous event (Neelin et al, 1998). Observations show that no frequency greater than 0.4 has been recorded in proxy El Niño records spanning thousands of years (Rodbell et al, 1999; Hughen et al, 1999). Since no obvious physical limit exists on the rates of change in T (perhaps as high as 10 °C/100yr at the close of the ice age) the appearance of saturation in El Niño suggests that global T is the independent variable in this relationship.

A stronger argument against the interpretation that El Niño is the independent variable is the short time required for the atmosphere to shed excess heat. As a general rule of thumb, atmospheric circulation and mean temperature can adjust to a new heat source within 14 days. This means that the effect of a heat source, which has been removed, does not persist for years. But, while the frequency of occurrence of El Niño events from the mid 1980's to late 1990's is not materially higher than that observed during the mid 1970's to mid 1980's, global T is. For the alternative hypothesis, that a large number of El Niño events have caused the rise in temperature, to be valid the heat from the El Niño events during the 1970's would have had to persist through the 1990's.

According to the evidence summarized in Fig. 2, when $dT/dt \approx 0$, the frequencies of El Niño and La Niña are both about 0.25/yr. The graphical symmetry suggests that, in the absence of climate change, the nonlinear feedback due to the coupling between the equatorial Pacific and tropical atmosphere is approximately equal for easterly wind anomalies, which can lead to La Niña, and for westerly wind anomalies, which can lead to El Niño (Neelin et al, 1998). With climate change however, the picture can be quite different. The third, and strongest, argument comes from a statistical investigation of the global temperature record itself.

3. Random walk analysis of global temperatures

According to random walk analysis, a time series $x(t)$ is mapped onto a walk by calculating the net displacement, $y(t)$, defined by the running sum

$$y(t) = \sum_{i=1}^{t} x(i).$$

A suitable statistical quantity used to characterize the walk is the root mean square fluctuation about the average displacement,

$$F(t) = [\langle [\Delta y(t)]^2 \rangle - \langle [\Delta y(t)] \rangle^2]^{1/2},$$

where $\Delta y(t) = y(t_0 + t) - y(t_0)$, and the averaging symbols ($\langle\ \rangle$) indicate an average over all positions, t_0, in the walk. When $F(t) \propto t^H$ it is possible to distinguish three types of behavior: (1) uncorrelated time series with $H = 0.5$, as expected from the central limit theorem, (2) time series exhibiting positive long-range correlations with $H > 0.5$, and (3) time series exhibiting negative long range correlations with $H < 0.5$. Markov processes with local correlations extending up to some scale also give $H = 0.5$ for sufficiently large t. It is well-known (Feder, 1988) that the correlation function $C(t)$ of future increments, $y(t)$ with past increments, $y(-t)$ is given by $C(t) = 2(2^{2H-1} - 1)$. For $H = 0.5$ we have $C(t) = 0$ as expected, but for $H \neq 0.5$ we have $C(t) \neq 0$ independent of t. This indicates infinitely long correlations and leads to a scale-invariance (scaling) associated with positive long-range correlations for $H > 0.5$ (i.e., an increasing trend in the past implies an increasing trend in the future) and with negative long-range correlations for $H < 0.5$ (i.e., an increasing trend in the past implies a decreasing trend in the future). Note however that positive long-range correlations do not imply persistence as usually used in climatology, which is defined as the continuance of a specific pattern over time. Scale invariance is a law that incorporates variability and transitions at all scales in the range over which it holds and is often a result of nonlinear dynamics. Of course, H is related to the spectra of the original time series $x(t)$ via a relationship of the form $P(f) \propto f^{-2H+1}$, where $P(f)$ is the power spectrum of frequency, f. Thus both $P(f)$ and $F(t)$ contain, in principle, the same information about the exponent H. However, $F(t)$ is superior for estimating H, because the definition of $F(t)$ involves averages over all positions, t_0, of the walk. $F(t)$ is a smoother function than $P(f)$. $P(f)$ fluctuates significantly, and as a result scaling regions are often masked. Because of that the estimation of slopes in $\log P(f)$ plots is not straightforward (Viswanathan et al, 1996). Note that long-term trends in $x(t)$ should be removed as they may correspond to processes at time scales longer than the length of the data. In these cases, the inclusion of a long-term trend will make the results trivial. Moreover, the effect of climate on ENSO at such long time scales was ascertained in the previous section (without subtracting out long-term trends), and the same general results were obtained as will be obtained next, that increases (reductions) in T induce more frequent El Niño (La Niña) occurrence. Thus the data of the previous section is complementary to the random walk analysis, in that the correlation

between dT/dt and El Niño frequency is demonstrated over different time scales and by different methods.

The actual definition of scaling demands that scaling extends to infinity (space or time). While this is possible in a mathematical sense, it is impractical in physical experiments or systems of any kind. Physical systems, like the climate, have finite size, and are characterized by processes that operate at different space/time scales (Tsonis, 1998). If these processes are scale invariant, the associated scaling must be limited. In such a framework, certain processes may promote a trend. This tendency can take the system away from its equilibrium state. Thus, it is reasonable to assume that if the system remains near equilibrium, processes must be operating at other time scales in order to avoid a runaway effect. Under this scenario we should be able to discover characteristic space or time scales associated with these mechanisms. Such characteristic scales provide useful insights about the system, which may enhance its predictability. The mapping of a time series to a random walk and the subsequent analysis provide an elegant way to search for characteristic time scales in data, as demonstrated next for global temperatures.

Figure 5a shows the actual monthly temperature anomaly record (also from Folland et al, 1990), and 5b the detrended anomaly record, $x(t)$. The trend is removed using singular spectrum analysis (SSA) (Elsner and Tsonis, 1996; Tsonis et al, 1998). Figure 5c shows the net displacement, $y(t)$, as a function of time. Figure 6 (circles) is a log–log plot of $F(t)$ vs. t for $0 \leq \log t \leq 2.4$ (1 month $\leq t \leq$ 20 years). As t approaches the sample size, the estimation of $F(t)$ involves fewer and fewer points. Thus, extending this type of analysis to longer time scales is not recommended (for more details see Tsonis et al, 1998).

The $\log F(t)$ function appears to exhibit two distinct linear regions separated by a small transition region: one in the interval $0 \leq \log t \leq 1.25$ ($1 \leq t \leq 18$ months) and another in the interval $1.35 \leq \log t \leq 1.95$ (22 months $\leq t \leq 7.4$ years). The linear fits over these two regions result in slopes $H_1 = 0.65$ and $H_2 = 0.4$. The correlation coefficient of the linear regression is in both cases greater than 0.99. The null hypothesis H_0:$H_1 = 0.5$ against the alternatives H_a:$H_1 > 0.5$ and the null hypothesis H_0:$H_2 = 0.5$ against the alternative, H_a:$H_2 < 0.5$ are both rejected at a significance level of 0.01. In order to show that the above result is not an artifact of the sample size,

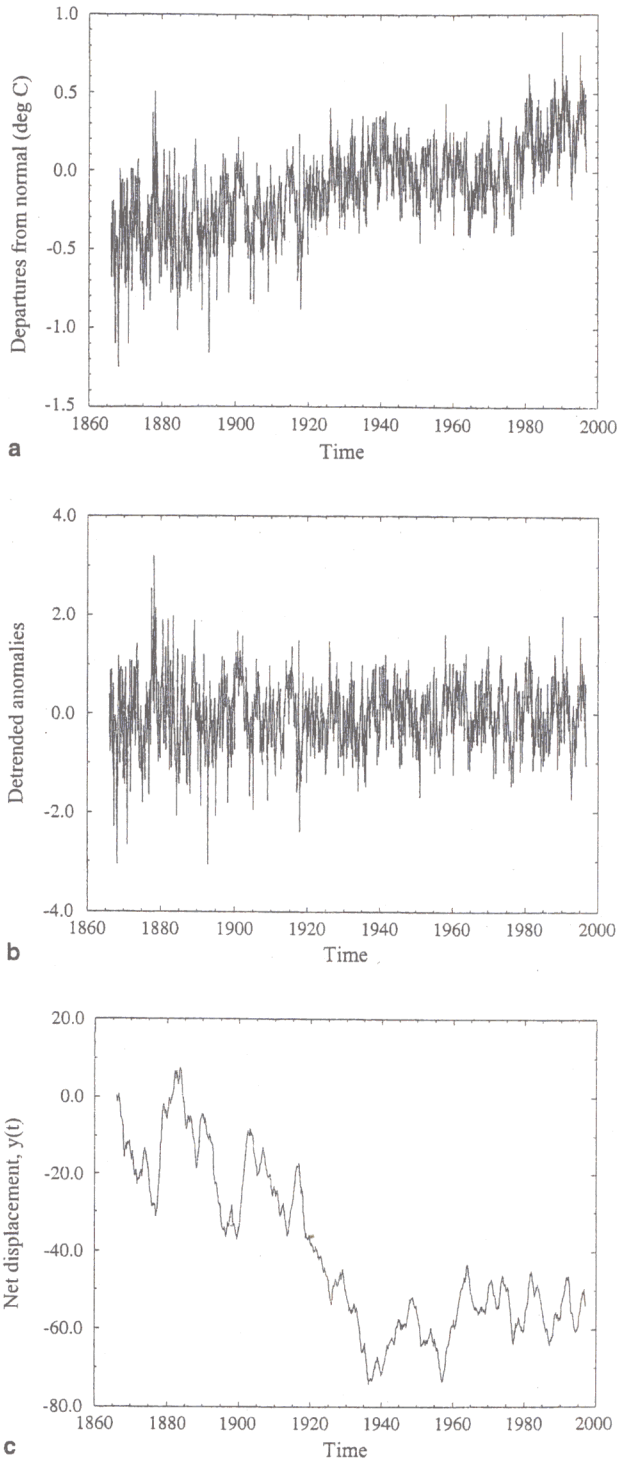

Fig. 5a. The IPCC monthly global temperature anomaly record (Folland et al, 1990); **b** The detrended monthly global temperature anomaly record, $x(t)$; **c** The net displacement, $y(t)$ of the random walk based on the data in 4b

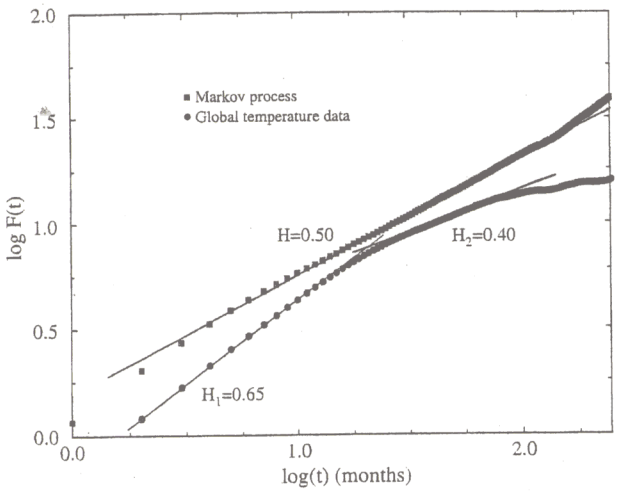

Fig. 6. The log–log plot of $F(t)$ vs. t. The circles correspond to the temperature data and the squares to a surrogate Markov process of the same length and lag one autocorrelation. The temperature data exhibit double scaling, whereas the stochastic data exhibit one scaling region as expected from theory

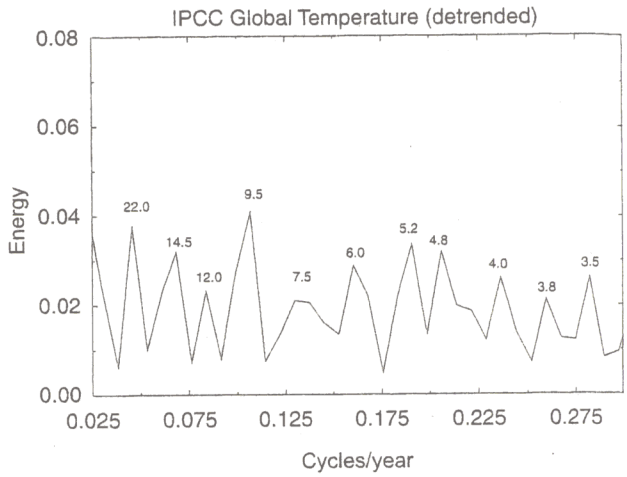

Fig. 7. The power spectrum of the IPCC temperature record. The peaks and the corresponding periodicities are in very good agreement with other approaches such as the multi-taper approach (see Ghil and Vautard, 1991)

we produce a Markov process with the same length and lag one autocorrelation as the temperature data and repeat the analysis. Now (squares in Fig. 6) the double scaling disappears, and we recover the expected slope of 0.5. The two linear regions in the log(F) function for the temperature data intersect at about $\log t = 1.3$ which corresponds to $t \approx 20$ months. Thus this analysis indicates that the data in Fig. 6 are consistent with a power law with $H_1 = 0.65$ for $t < 20$ months and with a power law with $H_2 = 0.4$ for $t > 20$ months. Alternatively stated, processes of time scales less than 20 months sustain a tendency toward an initial trend (whether positive or negative) and processes of time scales greater than 20 months tend to reverse the past trend. This change in scaling defines an important characteristic time scale in global climate.

The spectra of global temperature data (Fig. 7) contain significant power at frequencies corresponding to the ENSO cycle (time scales 3–7 years). This result is usually (and correctly) interpreted to imply that ENSO affects global temperatures. While 3–7 years covers most of the scaling range corresponding to negative correlations, the interpretation of the result is complex. As a response to, e.g., a rise in T, El Niño is made more likely. El Niño causes a further increase in T for the next 16 months or so, or as long as the western Pacific energy source has not been exhausted. Subsequently global temperatures cool off. Repetition of an El Niño at, say, 4 years, contributes to an oscillatory wave form of the global T record with a period of 4 years, contributing strongly to $P(f)$ at 1/4/yr. Beyond this, however, increases in T which persist for longer times trigger more frequent El Niños throughout the period.

An important point in understanding a random walk analysis of the global temperatures involves some basic aspects of El Niño physics. The western equatorial and off-equatorial Pacific, in contrast to the east, act as a large thermal reservoir (Neelin et al, 1998); in this region of the Pacific SST's are not in equilibrium with the wind stress, as they are in the eastern equatorial Pacific (Schneider et al, 1995). An El Niño event depletes this storage of heat, largely by spreading the heat over a much broader region of the sea surface, while simultaneously reducing the typical vertical thickness of the warm upper layer. As El Niño matures, the depth to the thermocline diminishes while latent heat is transferred to the atmosphere. After typically about 16 months, when the heat energy is depleted, the El Niño begins to collapse. Thus, any event, which triggers an El Niño tends to raise atmospheric temperatures for up to 16–18 months. Subsequently, however, the heat storage in the western Pacific is reduced, and it takes generally on the order of

two years to replenish, meaning that atmospheric temperatures are then typically reduced. In this light, the above result that atmospheric temperature fluctuations tend to be accentuated over time scales of up to 18 months, while they tend to be self-correcting on time scales of 2–7 years, has only one possible interpretation. For short periods of time, increases in atmospheric temperatures trigger El Niños. The development of an El Niño further increases atmospheric temperatures. After El Niño has run its course, the reduction in stored heat in the equatorial and off-equatorial Pacific leads to a reduction in atmospheric temperatures, and the heat reservoir in the tropical oceans is utilized by the ocean-atmosphere system for self-correction. An analogous argument holds for La Niña.

The mathematical interpretation of the random-walk results indicates a role for the ENSO cycle in balancing global temperature. Finally note that according to the formulation of the random walk analysis the above result does not depend on the actual temperature but on the temperature changes. This is consistent with our results and arguments presented in Sect. 2. Support for these suggestions is provided in Fig. 8, which shows the Southern Oscillation Index for the last 100+ years, and a three-year running average of global temperatures. A quick look demonstrates that in the past century three distinct periods of El Niño activity exist (see also Trenberth and Hoar, 1997). The first 25 years have $dT/dt > 0$, elevated El Niño occurrence, and suppressed La Niña activity. The next 50 years have $dT/dt \approx 0$, and more or less equal La Niña and El Niño activity. The final years mark a return to the conditions of the early 20th century with very high El Niño activity. Correlations between El Niño and dT/dt are also visible on shorter time scales. The random walk analysis, suggests that the role of ENSO is to moderate changes in global temperature, T. Thus, when T rises, the likelihood of triggering an El Niño is increased and the rise in T is either reversed or reduced. Precisely the opposite holds for La Niña. The tendency for ENSO to moderate climate change can be seen in 43 of the 65 events in the last 120 years. If yearly temperature values are substituted for the three-year average, 58 of the 63 events are consistent with the role of ENSO as a short-term moderator of climate change.

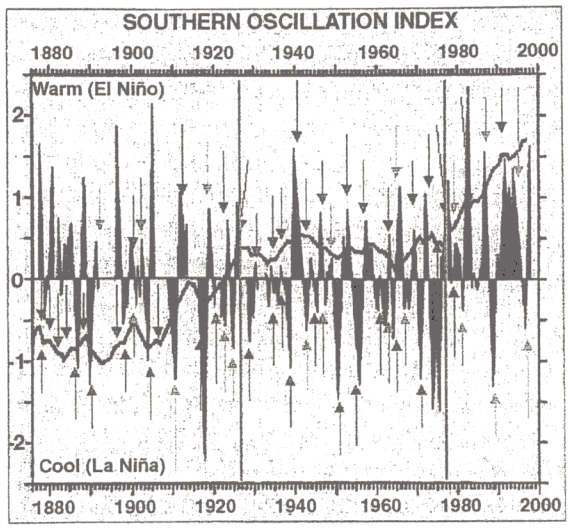

Fig. 8. Comparison of yearly SOI values with global temperature (Folland et al, 1990). The SOI is given by the vertical triangles. Note that in the SOI data (taken from NOAA's web pages) the signs have been reversed so that positive values indicate El Niño events and negative values La Niña events. The curve is a three-year running average of global temperatures. Upward pointing arrows signify La Niña, downward arrows, El Niño. Blue implies that the curvature of the global temperature at that event is appropriate considering the role of El Niño to try to reverse increases in T, La Niña to reverse reductions in T. Green implies the same, but for cases where it is only visible when the yearly T is plotted, rather than the multi-year average shown here. Red implies that the events do not have the expected moderation of global T fluctuations. The tendency for ENSO to moderate climate change can be seen in 43 of the 65 events in the last 120 years. If yearly temperature values are substituted for the three-year average, 58 of the 63 events are consistent with the role of ENSO as a short-term moderator of climate change. The two bold magenta vertical lines separate regimes of different dT/dt with significant changes in El Niño and La Niña occurrence frequencies

Our hypothesis is also consistent with recent studies that have suggested El Niño as a mechanism for the tropics to shed excess heat (Sun and Trenberth, 1998; UCAR Quarterly, 1997). According to this study, the continuous pouring of heat into the tropics cannot be sufficiently removed by weather systems and ocean currents. By considering global oceanic and atmospheric heat budgets during the 1986–1987 El Niño, they suggested that El Niño acts as a release valve for the tropical heat. This has also been confirmed from studies of other events (Sun, 2000; Sun, 2001, personal communication). In addition to these results, we cite the work of (1) Tsonis

and Elsner (1997) where, using methods from the theory of nonlinear dynamical systems, it was shown that global temperature trends and ENSO predictability are coherent over the Nyquist frequency band from 0.0 to 0.24 cycles/year. These results established a connection between global temperature and ENSO with increasing temperatures resulting in lower ENSO predictability. (2) Timmermann et al (1999b) where it is shown that the frequency of El Niño in a coupled ocean-atmosphere model was increased in a simulated global warming scenario. (3) Trenberth et al (2002) showed that the contribution of El Niño to the magnitude of the recent global warming is only 0.06 °C, which is less than 10% of the overall warming. This does not support the school of thought that it is El Niño that affects global temperature trends.

4. How do all these relate to key aspects of recent ENSO theories?

We will now discuss how our theory fits with the underlying physical mechanisms of El Niño triggering and development, predictability, and variability.

4.1 Triggering

As noted in the introduction, it is widely accepted that the trigger of El Niño is a combination of anomalous westerly wind bursts (Wyrtki, 1975; McPhaden, 1999; Yu and Rienecker, 1998), equatorial Pacific SST gradient, and a sufficient heat energy, which through the positive feedback of convection spreads around the surface of the entire equatorial Pacific (Neelin et al, 1998). Is this consistent with our hypothesis? We argue that it is because of the following: (1) An increase in global temperatures leads to rapid (and greater) heat storage in the tropical Pacific. This is supported by recent analyses which show that during the 20th century (a time of general global warming) the western equatorial Pacific warmed by 0.2 °C, while the eastern Pacific warmed by a smaller amount (Latif et al, 1997; Cane et al, 1997). Thus both the mean SST and the east–west gradient have increased. (2) Increased heat storage leads to stronger trade winds. This is also supported by data analyses (Latif et al, 1997; Shriver and O'Brien, 1995), which indicate that simultaneous with global temperature increases are increases in trade wind strength. (3) The accompanying increase in trade wind strength induces an increase in trade wind fluctuations. This follows from scaling arguments for turbulent flow in boundary layers, (Kolmogorov, 1941) and it is consistent with thermodynamic arguments: more energy into a system implies greater fluctuations (in fact for this to be not true the system must have negative temperatures). As such, the proposed hierarchy of influences in our hypothesis is consistent with the underlying physical mechanisms of El Niño development as inferred from the historical data. Note that from the arguments of Hunt (1999a), it appears that increased trade wind fluctuation would trigger both more El Niño and more La Niña events in contrast to what is observed (more El Niño events and fewer La Niña events). His argument, based on dynamics without consideration of the thermodynamics of global temperature fluctuations, misses the tendency for increasing global temperatures to suppress La Niña initiation. A qualitative argument to explain the suppression of La Niña events during rising temperatures can be constructed in line with the previous paragraph. With rapid storage of energy, the thermal and physical inertia of the regions of heat storage in the western Pacific should increase more rapidly, with the tendency for enhanced sea surface elevation gradients. Large sea surface elevation gradients suppress the trigger of La Niña, even when typical trade winds are strong *and* fluctuations are large. Finally, the fact that La Niña often follows El Niño is consistent with the evidence that El Niño depletes the oceanic heat storage and often triggers a subsequent drop in global atmospheric temperatures. By symmetry, El Niño often follows La Niña.

4.2 Predictability

An aggregate of forcing of El Niño through trade wind stress, spatial SST patterns and equatorial upwelling is responsible for the typical boreal spring onset of El Niño as suggested by Tziperman et al (1998). Looking at just one of the components of this aggregate, namely trade wind stress, we see that the Northern Hemisphere

trades are strongest in the boreal winter, when the Southern Hemisphere trades are weakest. Thus the power spectrum of zonally averaged trade wind forcing must have a contribution at a period of twelve months, and both the spring and fall are times of weaker trades. Due to asymmetries in the Pacific Ocean basin, the Northern Hemisphere spring is the time of greatest reduction in trade wind forcing, as well as of greatest reduction in cold water advection into the central Pacific, but since averaging effectively involves both Hemispheres, Fourier components at one year must be fairly small. This has been confirmed by Lagos et al (1987) who showed that the amplitude of the annual cycle harmonic of zonal wind in the central and western equatorial Pacific is indeed very small. Thus it is possible that rapid changes in global T, since they occur in both Hemispheres by definition, can produce changes in trade wind forcing at periods of six months or a year which are on the same order of magnitude as those which are most effective in triggering El Niño. Analogous arguments can be constructed for the influences of upwelling and SST's.

Consider a scenario with a moderate increase in global T, but which produces smaller changes in trade wind forcing than the seasonal cycle. Then the occurrence of El Niño should be enhanced, but the seasonality of the onset left unaffected. If, on the other hand, the increase of global T is very rapid, it should be possible to produce six-month variations in trade wind strength, which are larger than the harmonics arising from the seasonal variability. In such a case, the seasonality (referred to as seasonal locking) of the initiation of El Niño could be destroyed. Balmaseda et al (1995) conclude, in fact, that in the period 1976–1989 the seasonal locking of El Niño was missing, in contrast to both the decade before 1976 and the period since 1990 (see also Mitchell and Wallace, 1996). Comparison with global temperature data shows that this period had perhaps the most rapid rise of temperature on the record, while the rise in T since the late 1980's has moderated. Interestingly enough, such a reduction in the role of the spring barrier to prediction actually enhanced the predictability of El Niño, since the spring barrier is the most difficult to overcome. Thus the TOGA decade may have been unusually impacted by the exceptionally rapid rise of global temperatures occurring during that period, and the modeling community may have been somewhat misled. The return to increased role of seasonal locking in the 1990's has contributed to degradation in predictive skill in most of the models (Latif et al, 1998; Chen et al, 1995; 1998).

4.3 Variability

Here we wish to discuss an issue that we think is of importance in the growing debate of El Niño/La Niña variability. In the ENSO community there seems to exist two distinct opinions. On one side there are those who believe that ENSO has its own internal complex nonlinear dynamics and that external influences are not crucial (in addition to earlier cited references, Gu and Philander (1997), Jin et al (1994), Tziperman et al, 1994; 1997; Neelin and Latif, 1998, should be mentioned). On the other side there are those who argue for a stochastic scenario where external forcing, such as trade wind fluctuations, are more important (Penland and Matrosova, 1994, for example). In this "internal/nonlinear vs. external influence/stochastic" controversy (and we do not mean to imply there is no middle ground), our results would seem to favor the latter. Yet, a closer examination of the present results suggests that the two opinions converge. Our approach certainly implies the relevance of T as a forcing function, but it does not require that T be regarded as a stochastic input to an, otherwise, independent ENSO system (although it may be convenient to regard it as so).

In the earth's climate system, which is spatially extended, it is reasonable to expect that subsystems exist at various space/time scales. Each of these subsystems describes a phenomenon at those space/time scales and exhibits its own dynamics. These subsystems are interconnected and thus exchange information (Tsonis and Elsner, 1989; Lorenz, 1991; Tsonis, 1996; Tsonis and Elsner, 1998). As an example we offer the interaction between convection and mid-latitude cyclones. The equations that describe the formation of a cumulonimbus cloud form a subsystem operating at certain space/time scales. The equations that describe the formation of mid-latitude cyclones also form a subsystem operating at longer

space/time scales. In physical terms, the synoptic arrangement determines the potential temperature field and the moisture convergence, which in turn affect cumulonimbus formation. The potential temperature field and moisture convergence are part of the information provided by the larger subsystem to the smaller subsystem. Similarly, the latent heat release in cumulonimbus development, which can affect cyclogenesis, is information provided by the smaller subsystem to the larger subsystem. The amount of information exchanged by a subsystem and the rest of the system is determined by the degree of connectivity. The degree of connectivity determines the degree of "communication" of a given system to the rest of the systems. If the degree of connectivity is small one can assume that the subsystem is independent and simply obeys its own dynamics. On the other hand if the amount of information provided to the subsystem from the system is significant, then the external influences affect the dynamics of the subsystem, and the system can appear stochastic. In fact, Tsonis and Elsner (1997) have presented evidence on how the predictability of the ENSO subsystem may be affected by the global temperature signal.

In the above mathematical framework the two views about ENSO converge. When the global temperature is constant, or nearly so, El Niño behaves as an independent system but when global temperature changes rapidly, it reacts accordingly. This is suggested by the data. In the case of relatively static temperatures, El Niño appears to be well-described by a deterministic, nearly linear model; the regularity of occurrence between 1941 and 1970 could have allowed predictability almost without understanding of the dynamics, e.g., 1940–42, 1946, 1952, 1958, 1965, 1969. Subsequently the situation changed as El Niño appears to behave more "randomly". Therefore, the complexity of El Niño, both in terms of its yearly variability and its seasonality, is enhanced by periods of rapid temperature rise, consistent with the proposed influence of rising T on the frequency of El Niño occurrence. From the above view, it could thus be suggested that the physical reasoning behind the dependence of this frequency on dT/dt rather than T, is the transient response of the ENSO system to external fluctuations of T.

5. Conclusions

We have presented mathematical and physical evidence that support the hypothesis that the occurrence and variability of El Niño are sensitive to changes in global temperatures, but not to the actual value of the global temperature. More specifically, our theory suggests that El Niño is activated to reverse positive global temperature trends, and La Niña to reverse negative trends. This makes global temperature *change* (which can be a result of natural variability and/or of increased greenhouse gases) an important input into the variability of El Niño. Thus, predictions of global temperature trends are of paramount importance to the forecasts of weather patterns during the 21st century.

Acknowledgments

AAT was partly supported by NSF grant ATM-9727329 and JBE was partly supported by NSF grant ATM-94-17528.

References

Anderson DM (1992) Long-term changes in the frequency of occurrence of El Niño events. In: El Niño: Historical and paleoclimatic aspects of the Southern Oscillation (Diaz H, Markgraf V, eds.), Cambridge University Press, pp 193–200

Balmaseda MA, Davey MK, Anderson DLT (1995) Decadal and seasonal dependence of ENSO prediction skill. J Climate 8: 2705–2715

Blanke B, Neelin JD, Gutzler D (1997) Estimating the effect of stochastic wind forcing on ENSO irregularity. J Climate 10: 1473–1486

Chen D, Zebiak SE, Busalacchi AJ, Cane MA (1995) An improved procedure for El Niño forecasting: Implications for predictability. Science 269: 1699–1703

Chen D, Cane MA, Zebiak SE, Kaplan A (1998) The impact of sea-level data assimilation on the Lamont model prediction of the 1997–1998 El Niño. Geophys Res Lett 25: 2837–2840

Collins M (2000) The El Niño-Southern Oscillation in the second Hadley Centre coupled model and its response to greenhouse warming. J Clim 13: 1299–1312

Elsner JB, Tsonis AA (1996) Singular spectrum analysis: A new tool in time series analysis plenum, New York

Evans MN, Fairbanks RG, Rubenstone JL (1999) The thermal oceanographic signal of El Niño reconstructed from Kiritimati Island coral. J Geophys Res-Oceans 104: 13409–13412

Feder J (1988) Fractals. New York: Plenum

Folland CK, Karl TR, Ya Vinnikov K (1990) Observed climate variations and change. In: Climate Change: The IPCC Scientific Assessment (Houghton JT,

Jenkins GI, Ephramus JJ, eds). Cambridge Univ. Press, pp 195–238
Ghil M, Vautard R (1991) Interdecadal oscillations and the warming trend in global temperature time series. Nature 350: 324–327
Gu D, Philander SGH (1997) Interdecadal climate fluctuations that depend on exchange between the tropics and the extra-tropics. Science 275: 805–807
Hughen KA, Schrag DP, Jacobsen SB (1999) El Niño during the last interglacial period recorded by a fossil coral from Indonesia. Geophys Res Lett 26: 3129–3132
Hunt AG (1999a) Understanding a possible correlation between El Niño occurrence frequency and global warming. Bull Amer Meteorol Soc 80: 297–300
Hunt AG (1999b) A physical interpretation of the correlation between El Niño and global warming, Proc. 24th NOAA Workshop on Climate Diagnostics and Prediction, Tucson, Arizona, November 5–9, 1999, pp 33–36
Hunt AG (2000) A stochastic atmospheric trigger for El Niño: Implications for east Pacific rise in seismicity. EOS 81: 272
Jin F-F, Neelin JD, Ghil M (1994) El Niño on the devil's staircase: Annual subharmonic steps to chaos. Science 264: 70–72
Kestin TS, Karoly DJ, Yano J-I, Rayne NA (1998) Time-frequency variability of ENSO and stochastic simulations. J Clim 11: 2258–2272
Kolmogorov AN (1941) Dissipation of energy in locally isotropic turbulence, Dokl. Akad. Nauk SSSR-32 16–18; reprinted in Proc. R Soc Lond A 434: 15–17 (1991)
Lagos P, Michell TP, Wallace JM (1987) Remote forcing of sea-surface temperature in the El Niño region. J Geophys Res-Oceans 92: 14,291–14,296
Latif M, Kleeman R, Eckert C (1997) Greenhouse warming, decadal variability or El Niño? An attempt to understand the anomalous 1990's. J Clim 10: 2221–2239
Latif M, Anderson D, Barnett T, Cane M, Kleeman R, Leetma A, O'Brien JJ, Rosati A, Schneider E (1998) A review of the predictability and prediction of El Niño. J Geophys Res 103: 14375–14393
Lorenz EN (1991) Dimension of weather and climate attractors. Nature 353: 241–244
McPhaden MJ (1999) The child prodigy of 1997–1998. Nature 398: 559–562
Mitchell TP, Wallace JM (1996) An observational study of ENSO variability in 1950–78 and 1979–92. J Clim 9: 3149–3161
Neelin JD, Battisti DS, Hirst AC, Jin F-F (1998) ENSO theories. J Geophys Res 103: 14261–14290
Neelin JD, Latif M (1998) El Niño dynamics. Physics Today 51: 32–36
Penland C, Matrosova L (1994) A balance condition for stochastic numerical models with applications to the El Niño-Southern Oscillation. J Clim 7: 1352–1372
Philander SG (1990) El Niño, La Niña and the Southern Oscillation. San Diego: Academic Press
Pollack HN, Huang S (1998) Underground temperatures reveal changing climate. Geotimes 43: 16–19
Quinn WH (1992) A study of Southern Oscillation-related climatic activity for AD 622-1900 incorporating Nile River flood data. In: El Niño: Historical and paleoclimatic aspects of the Southern Oscillation (Diaz H, Markgraf V, eds). Cambridge University Press, pp 119–150
Rajagopalan B, Lall U, Cane MA (1997) Anomalous ENSO occurrence: An alternate view. J Clim 10: 2351–2357
Rodbell DT, Seltzer GD, Anderson DM, Abbott MB, Enfield DB, Newman JH (1999) An ~15,000 year record of El Niño driven alluviation in southwestern Ecuador. Science 283: 516–520
Schneider EK, Huang B, Shukla J (1995) Ocean wave dynamics and El Niño. J Clim 8: 2415–2439
Shriver JF, O'Brien JJ (1995) Low frequency variability of the equatorial Pacific Ocean using a new pseudostress dataset: 1930–1989. J Clim 8: 2762–2786
Solow AR (1995) Testing for change in the frequency of El Niño events. J Clim 8: 2563–2566
Sun D-Z (2000) The heat sources and sinks of the 1986–87 El Niño. J Clim 13: 3533–3550
Sun D-Z, Trenberth K (1998) Coordinated heat removal from the equatorial Pacific during the 1986–87 El Niño. Geophys Res Lett 25: 2659–2662
Timmermann A, Latif M, Grotzner A, Voss R (1999a) Modes of climate variability as simulated by a coupled general circulation model. Part I: ENSO-like climate variability and its low-frequency modulation. Clim Dyn 15: 605–618
Timmermann A, Oberhuber J, Bacher A, Esch M, Latif M, Roeckner E (1999b) Increased El Niño frequency in a climate model forced by future greenhouse warming. Nature 398: 694–696
Trenberth KE, Hoar TJ (1997) El Niño and climate change. Geophys Res Lett 24: 3057–3060
Trenberth KE, Caron JM, Stapaniak DP, Worley S (2002) Evolution of El Niño-Southern Oscillation and global atmospheric surface temperatures. J Geophys Res 107: D8(10.1029/2000JD000298)
Tsonis AA (1996) Dynamical systems as models for physical processes. Complexity 1: 23–33
Tsonis AA (1998) Fractality in nature. Science 279: 1614–1615
Tsonis AA, Elsner JB (1989) Chaos, strange attractors, and weather. Bull Amer Meteor Soc 70: 16–23
Tsonis AA, Elsner JB (1997) Global temperature as a regulator of climate predictability. Physica D 108: 191–196
Tsonis AA, Elsner JB (1998) Comments on "The southern oscillation as an example of a simple ordered subsystem of a complex chaotic system". J Climate 11: 2453–2454
Tsonis AA, Roebber PJ, Elsner JB (1998) A characteristic time scale in the global temperature record. Geophys Res Lett 25: 2821–2823
Tziperman E, Stone L, Cane MA, Jarosh H (1994) El Niño chaos: Overlapping of resonances between the seasonal cycle and the Pacific ocean-atmosphere oscillator. Science 264: 72–74
Tziperman E, Scher H, Zebiak SE, Cane MA (1997) Controlling spatio-temporal chaos in a realistic El Niño prediction model. Phys Rev Lett 79(6): 1034–1037
Tziperman E, Cane MA, Zebiak SE, Xue Y, Blumenthal B (1998) Locking of El Niño's peak time to the end of the calendar year in the delayed oscillator picture of ENSO. J Climate 11: 2191–2199

UCAR Quarterly El Niño and global warming: what's the connection (UCAR office of programs, vol. 24 winter, 1997)

Viswanathan GM, Afanasyev V, Buldyrev SV, Murphy EV, Prince PA, Stanley HE (1996) Levy flight search patterns of wandering albatrosses. Nature 381: 413–415

Walker GT (1923) Correlation in seasonal variations of weather III: A preliminary study of worldwide weather. Mem Indian Meteorol Dep 24: 75–131

Walker GT (1924) Correlation in seasonal variations of weather IX: A further study of world weather. Mem Indian Meteorol Dep 24: 275–332

Wang B, Wang Y (1996) Temporal structure of the Southern Oscillation as revealed by waveform and wavelet analysis. J Climate 9: 1586–1598

Wyrtki K (1975) El Niño – The dynamic response of the equatorial Pacific Ocean to atmospheric forcing. J Phys Oceanogr 5: 542–584

Yu LA, Rienecker MM (1998) Evidence of an extratropical atmospheric influence during the onset of the 1997–98 El Niño. Geophys Res Lett 25(18): 3537–3540

Authors' addresses: A. A. Tsonis, Department of Mathematical Sciences, Atmospheric Sciences Group, University of Wisconsin-Milwaukee, Milwaukee, WI 53201-0413, USA (E-mail: aatsonis@uwm.edu); A. G. Hunt, CIRES, University of Colorado, Boulder, CO 80309, USA; J. B. Elsner, Department of Geography, Florida State University, Tallahassee, FL 32306, USA